RSC Advances

COMMUNICATION

View Article Online
View Journal | View Issue

Cite this: *RSC Adv.*, 2015, **5**, 88710

Received 18th May 2015
Accepted 14th October 2015

DOI: 10.1039/c5ra09250g

www.rsc.org/advances

Pharmacological evaluation of hybrid thiazolidin-4-one-1,3,5-triazines for NF-κB, biofilm and CFTR activity

Jitendra Kumar Srivastava,†[a] Nikhil T. Awatade,†[b] Hans Raj Bhat,[a] Arthur Kmit,[c] Karina Mendes,[b] Margarida Ramos,[b] Margarida D. Amaral[b] and Udaya Pratap Singh*[a]

Cystic fibrosis (CF) is a monogenetic disease caused mostly by the F508del mutation, a deletion of phenylalanine at position 508 of the CF transmembrane conductance regulator (CFTR) protein, which causes improper localization and functioning of this chloride channel in lung, pancreas, and intestine by affecting the normal fluid homeostasis. In CF the lungs are the most affected organ due to the accumulation of thick mucus, which results into heavy bacterial load and associated chronic inflammation. Therefore, novel state-of-the-art therapies are needed to circumvent this problem. To address this, a series of compounds (thiazolidin-4-one-1,3,5-triazines) was tested for the inhibition of NF-κB, and compounds SP6 and SP5 showed most significant activity (respectively with relative NF-κB activity: 1.82 ± 1.87 and 1.96 ± 1.56). Docking studies of the active compounds in the DNA binding surface of the N-terminal domains of NF-κB were also carried out to identify which structural motifs are vital for activity. These compounds were also tested for antibiofilm activity against *P. aeruginosa* and *S. aureus* where they showed MIC ranges from 7.81–125 μg mL^{-1}. The most active compound – SP6 was further assayed by micro-Ussing chamber experiments to determine its CFTR inhibitory properties, given its structural similarity to CFTR Inh_{172}. Results suggest that SP6 does not inhibit CFTR alone or in combination with Inh_{172}.

Introduction

Cystic fibrosis (CF) is the most common lethal monogenic disease caused by inherited mutations in a gene that encodes the CF transmembrane conductance regulator (CFTR) protein. The product of this gene is a plasma membrane protein with chloride (Cl^-) channel function which is mainly expressed in the apical membrane of epithelial cells in the airways, pancreas, intestine, and testes. Although CFTR functions mainly as a Cl^- channel, it has many other regulatory roles, including inhibition of sodium (Na^+) transport through the epithelial Na^+ channel (ENaC) which controls the hydration level of airway surface liquid (ASL) and thus also normal ciliary clearance (MCC) of mucus.[1]

The absence of CFTR function also results in an inherent hyper-inflammatory lung phenotype causing chronic obstructive lung disease which is characteristic of CF.[2] In addition to its well documented Cl^- channel function, it is evident that CFTR has other critical signalling and/or transport functions directly or indirectly associated with chronic inflammation. As a consequence, mucociliary clearance (MCC) is impaired, leading to chronic bacterial airway infections mostly caused by *Pseudomonas aeruginosa*. The characteristic of CF airway pathology is the elevated secretion of several pro-inflammatory cytokines where *P. aeruginosa* products have been reported to interact with Toll-like and asialo GM1 receptors expressed on bronchial epithelial cells, leading to downstream activation of nuclear transcription factors, including transcription factor nuclear factor kappa B (NF-κB).[3] Early studies indicated that genetic mutations in CFTR may be a risk factor for chronic lung diseases such as chronic obstructive lung disease (COPD) or asthma.[4a] More recently, cigarette smoke has been shown induce lack of functional CFTR at the cell surface,[4b,c] and patients with COPD were shown to display a similar defect, leading some authors to consider CCOPD as acquired CFTR deficiency.[4d,e]

The strategy for preventing progressive reduction of lung function in CF patients could be achieved by three different approaches, namely: (a) CFTR correctors and potentiators to increase CFTR plasma membrane levels/activity; (b) antibiotic drugs to treat/inhibit bacterial infections and (c) drugs used to control chronic inflammatory condition (*e.g.*, NF-κB inhibitors). Among the latter inhibitor class, triazine, coumarin, and quinazoline scaffolds interact directly with one or more of the NF-κB family proteins to

[a]*Drug Design & Discovery Laboratory, Department of Pharmaceutical Sciences, Sam Higginbottom Institute of Agriculture, Technology & Sciences, Allahabad, India. E-mail: udaysingh98@gmail.com*

[b]*University of Lisboa, Faculty of Sciences, BioISI – Biosystems & Integrative Sciences Institute, Campo Grande, 1749-016 Lisboa, Portugal*

[c]*Faculdade de Ciências Médicas - Universidade Estadual de Campinas R. Tessália Vieira de Camargo, 126. Cidade Universitária "Zeferino Vaz" CEP: 13083-887, Campinas, SP, Brazil*

† Equal contribution.

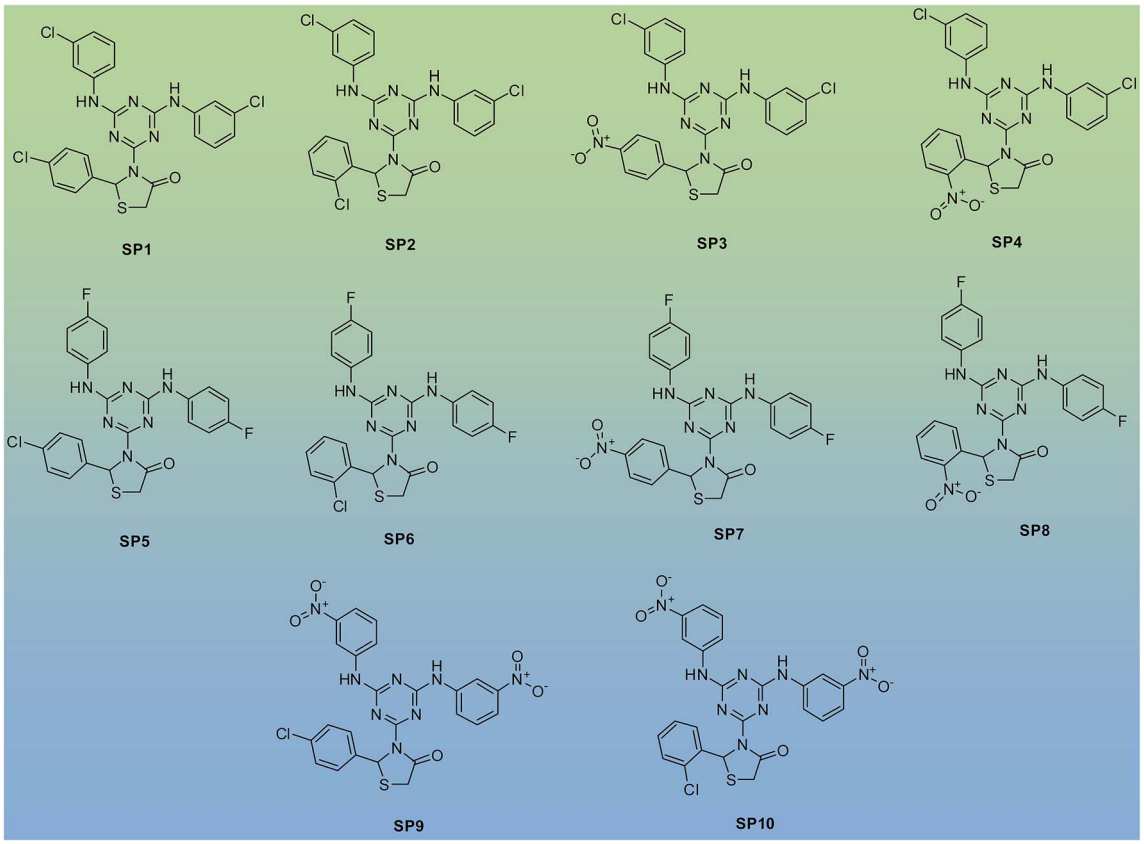

Fig. 1 Structures of hybrid thiazolidin-4-one-1,3,5-triazines used in the present study.

prevent DNA binding.[5] The inhibition of bacterial infections by antibiotics in turn would control infection and consequently its associated inflammatory response.

We have previously developed a series of thiazolidin-4-one-1,3,5-triazines and thiazolidine-2,5-dione-1,3,5-triazine as potent antibacterial agents (Fig. 1)[6] and here we have tested a series of thiazolidin-4-one-1,3,5-triazines (synthesis reported elsewhere)[6c] for possible inhibition of NF-κB and to determine the effect on the CFTR channel in primary human bronchial epithelial cells derived from patient's lung explants.

Material and methods

Development of novel hybrid molecules

The hybrid molecules selected for this study was synthesized earlier by our group with the help of novel one-pot, multi-component reaction strategy, where entire starting materials were taken in single pot. These compounds were furnished *via* efficient condensation–cyclisation reaction in excellent yield as described elsewhere.[6c]

NF-κB transcriptional activity

RAW264.7 macrophages were purchased from American Type Culture Collection (ATCC, USA). Cells were cultured in DMEM with 10% FBS, 100 mg mL^{-1} streptomycin and 100 U mL^{-1} penicillin in humidified 5% CO_2 at 37 °C.

The 80% confluency of RAW264.7 cells was achieved in six-well plates and transfected with 1 μg of the NF-κB reporter construct, along with 0.5 μg of pSVGal plasmid using Lipofect-AMINE 2000 (Invitrogen) in Opti-MEM medium (Gibco). After 24 hours of transfection, cells were treated with LPS or target derivatives (100 μM) for an additional 2 hours, and then lysed using the reporter lysis buffer (Promega). Luciferase assays were performed using 20 mL of cell extract and 100 mL of luciferin substrate (Promega), and the luciferase activity was measured using a Dual-Luciferase Reporter Assay System (Promega) according to the manufacturer's instructions. Data are normalized for transfection efficiency by dividing firefly luciferase activity with that of Renilla luciferase.[10]

Docking study

The docking of the most active compound (SP-6) was performed with p50 NF-κB (1nfk.pdb) using the LigandFit module of the Discovery Studio 2.5 (Accelrys Software Inc., San Diego; http://www.accelrys.com).

Ligand preparation

Using the built-and-edit module of DS 2.5, various ligands were built all-atom CHARMm force field parameterization was assigned, and then minimized using the ABNR method. A conformational search of the ligand was carried out using a stimulated annealing molecular dynamics (MD) approach.

The ligand was heated to a temperature of 700 K and then annealed to 200 K. Thirty such cycles were carried out. The transformation obtained at the end of each cycle was further subjected to local energy minimization, using the ABNR method. The 30 energy-minimized structures were then superimposed and the lowest energy conformation occurring in the major cluster was taken to be the most probable conformation.

Receptor preparation

The target receptor for the study was taken and the bond orders were corrected. The hydrogen atoms were added, and their positions were optimized using the all-atom CHARMm (version c32b1) force field with Adopted Basis set Newton Raphson (ABNR) minimization algorithm, until the root mean square (r.m.s) gradient for potential energy was <0.05 kcal mol^{-1} $Å^{-1}$. Using the 'Binding Site' tool panel available in DS 2.5, the minimized crystal structure of p50 NF-κB homodimer was defined as receptor, and binding site has been identified by built-in protocol. The side chains of the residues in the binding site were assumed to be flexible during refinement of post-dock poses. Once the receptor binding site was defined, it was then used for the docking studies. Using the built-and-edit module of DS 2.5, various ligands were built; all-atom CHARMm force field parameterization was assigned, and then minimized using the ABNR method. A conformational search of the ligand was carried out using a stimulated annealing molecular dynamics (MD) approach. The ligand was heated to a temperature of 700 K and then annealed to 200 K. Thirty such cycles were carried out. The transformation obtained at the end of each cycle was further subjected to local energy minimization, using the ABNR method. The 30 energy-minimized structures were then superimposed and the lowest energy conformation occurring in the major cluster was taken to be the most probable conformation.

After preparation of receptor and ligand, docking of SP6 was carried out using the LigandFit module. This docking algorithm combines a shape comparison filter with a Monte Carlo conformational search to generate docked poses consistent with the binding site shape. These initial poses were further refined by rigid body minimization of the ligand with respect to the grid based calculated interaction energy using the Dreiding force field.[11] The receptor protein conformation was kept fixed during docking, and the docked poses were further minimized using all-atom CHARMm force field and smart minimization method (steepest descent followed by conjugate gradient), until r.m.s gradient for potential energy was <0.05 kcal mol^{-1} $Å^{-1}$. The atoms of ligand and the side chains of the residues of the receptor within 5 Å from the center of the binding site were kept flexible during minimization.

Antibiofilm activity

For antibiofilm activity evaluation, overnight cultures of *S. aureus* (NCIM-2079) and *P. aeruginosa* (NCIM-2036) were diluted 1 : 10 in TSB (OD_{600} = 0.6–0.8) and then diluted to 1 : 200 in MH. The bacterial suspension was inoculated into the wells of sterile 96-well polystyrene microtiter plates incubated at 37 °C for 6 h.

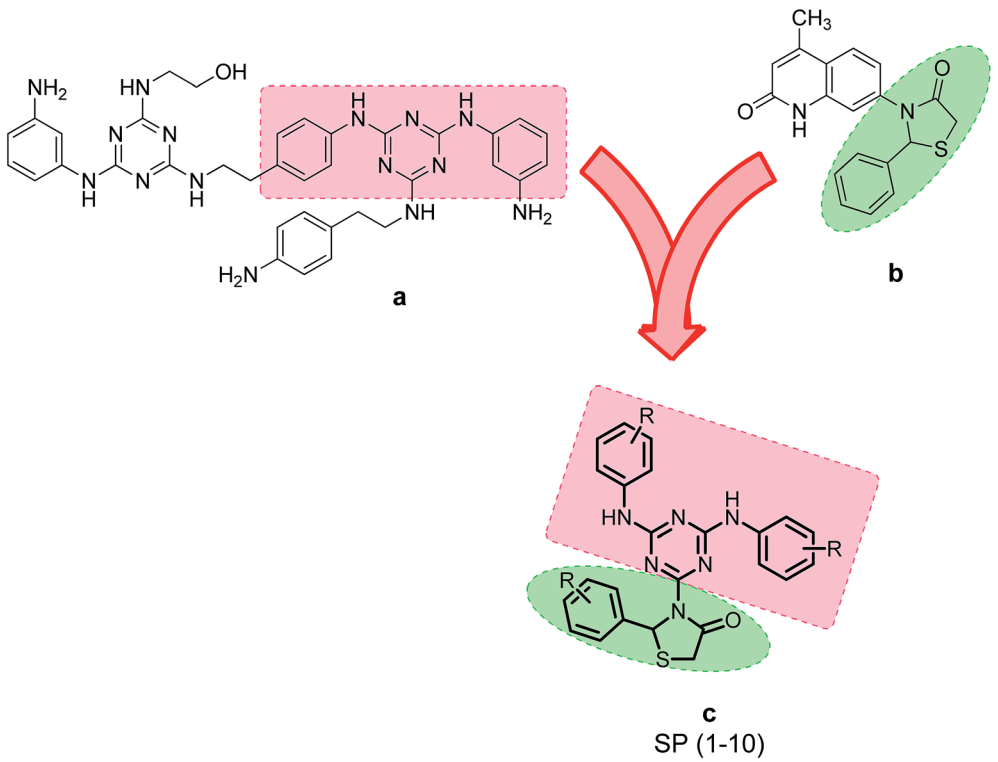

Fig. 2 Designing of target molecules *via* molecular hybridization strategy (MHS), where (a) PBI-1308, (b) substituted thiazolidin-4-ones, (c) hybridized target structure SP (1–10).

The plates with young biofilm were washed gently four times with sterile PBS before adding fresh TSB containing the various concentrations of compounds, and incubated at 37 °C for 16 h.[6a] The plates were washed again with PBS, and 99% methanol was added for 15 min. Whereas, well containing the young biofilm was washed by sterile PBS then dried. This well served as negative control and this value was deducted from the experimental readings. Another well containing young biofilm, sterile TSB was added and served which served as positive control. Each assay was performed in triplicate and the MIC of the compounds was according to the broth micro dilution (in tubes) method.

Effect on CFTR activity

Primary cultures of human bronchial epithelial (HBE) cells were isolated as described previously[13] and then expanded and grown on collagen IV-coated porous membranes (Snapwell, Corning-Costar®, Tewksbury, MA, USA) also as described.[14] Transepithelial electrical resistance (TEER) of the HBE monolayers grown on porous membranes was measured with the chopstick electrode (STX2 from WPI®, Berlin, Germany) and electrophysiological analyses were carried out in monolayers with resistance values above 600 Ω cm^2. Monolayers of polarized primary HBE cells grown on filters were mounted in perfused micro-Ussing chambers and analysed under open-circuit conditions at 37 °C, as before.[15] Values for the transepithelial voltage V_{te} were referenced to the basal surface of the epithelium. Transepithelial resistance R_{te} was determined by applying 1 s current pulses of 0.5 μA (5s-period). The cAMP-stimulated CFTR equivalent short-circuit currents ($I_{eq\text{-}sc}$) were calculated according to Ohm's law from V_{te} and R_{te} ($I_{eq\text{-}sc} = V_{te}/R_{te}$), with appropriate correction for fluid resistance. Ringer solution Cl^- concentrations apical and basal were 30 mM and 145 mM respectively, and pH adjusted to 7.4. Following a 20 min equilibrium period, amiloride (20 μM) added to the luminal side to block epithelial Na^+ channel (ENaC)-mediated Na^+ flux, then cAMP agonist, 2 μM forskolin (Fsk), the CFTR potentiator 25 μM genistein (Gen), and the CFTR channel blocker CFTR Inh_{172} (30 μM) or SP6 test compound (at 30, 40, 50 μM) were added sequentially.

All experiments were performed in compliance with the relevant laws and institutional guidelines, and that informed consent was obtained for any experimentation with human subjects (*e.g.* in providing bronchial epithelial cells), and Hospital Ethics committee of University of Lisbon, Portugal have approved the experiments.

Results and discussion

Development of novel hybrid molecules

The development of hybrid molecules was based on the molecular hybridization strategy, where two different independent active compounds are combined into one covalently linked hybrid compounds. The main advantage of this strategy is the synergistic effects of both moieties, which leads to the enhancement of pharmacological activity than individual component. These compounds are highly suitable for treatment of multifactorial disease by simultaneously hitting numerous targets for an indentified disease. The best examples of these compounds are utilized against Alzheimer's disease, PI3K/AKT/mTOR as anticancer, epidermal growth factor signalling cascade, or as antimalarial agent *via* simultaneously acting on different target. On the other hand, incorporation of two chemical moiety into single scaffolds is quite tedious and cumbersome process, and this could be overcome by utilizing multi-component approach *via* one-pot synthesis. Thus, compounds used in present study was synthesized using the same approach by combining two diverse pharmacophores and the selection is based on their earlier reported pharmacological activities. It was evident that, PBI-1308, a dimeric 1,3,5-triazine molecule developed by ProMetic BioSciences (Canada) significantly inhibits the inflammation *via* inhibition of NF-κB, Fig. 2(a).[8] Results showed that, PBI-1308 inhibits NF-κB in a dose dependent manner. In contrast, thiazolidin-4-one, an another important pharmacophore proved to exhibit potent anti-inflammatory action, Fig. 2(b).[9] Hence, development of new chemical entity that incorporate these vital anti-inflammatory pharmacophores, *i.e.*, 1,3,5-triazine and thiazolidin-4-one into a single chemical skeleton may further enlarge the spectrum of the activity, Fig. 2(c).

Table 1 Effect of hybrid derivatives on NF-κB transcriptional activity in LPS-stimulated RAW264.7 cells[a]

Analogue	Relative NF-κB activity (NF-κB/TK, fold)
SP1	$2.45 \pm 0.34^{\#\#}$
SP2	$2.26 \pm 1.23^{\#\#}$
SP3	$3.88 \pm 2.35^{\#\#}$
SP4	$3.12 \pm 0.78^{\#\#}$
SP5	$1.96 \pm 1.56^{\#\#}$
SP6	$1.82 \pm 1.87^{\#\#}$
SP7	$2.74 \pm 0.67^{\#\#}$
SP8	$2.45 \pm 0.12^{\#\#}$
SP9	$5.12 \pm 0.33^{\#\#}$
SP10	$4.77 \pm 1.46^{\#\#}$
Control	1.22 ± 0.34
LPS	$5.15 \pm 0.75^{**}$

[a] $N = 3$. $^{**}P < 0.01$ *vs.* control. $^{\#\#}P < 0.01$ *vs.* LPS.

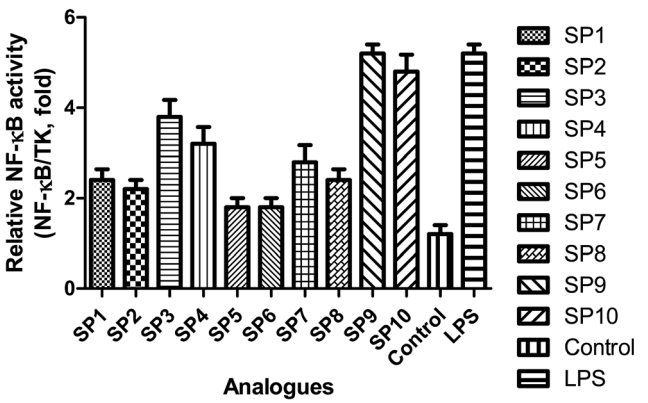

Fig. 3 Relative NF-κB activity of designed analogues.

Inhibitory effect on NF-κB activation

Once challenged by bacterial infection, a high concentration of pro-inflammatory cytokines – tumor necrosis factor-alpha (TNF-α), IL-1β, IL-6, IL-8, and granulocyte-macrophage colony-stimulating factor –is found in bronchoalveolar lavage fluid (BALF) of CF patients. All these proinflammatory cytokines have the common characteristic that their synthesis is promoted by NF-κB. NF-κB, a dimeric protein belongs to a family of transcription factors (Rel/NF-κB). In most cell types, it is sequestered in the cytoplasm by specific IκB proteins. Upon stimulation by different stimuli such as microbial products, proinflammatory cytokines, T- and B-cell mitogens, and physical and chemical stresses, IκB is phosphorylated by IKK, the IκB kinase, on two serine residues located within a conserved motif. This conversion activates the polyubiquitination of IκB by an ubiquitin ligase complex, and further leads to degradation by the 26S proteasome. The resulting free NF-κB translocates into the nucleus, where it binds to the target DNA (κB sites), and initiates or represses a large collection of target genes.[7] Accordingly, a direct attack on inflammation by inhibition of NF-κB would provide relief to the CF patients by preventing the generation of various mediators which are responsible for significant pathology in the CF lung.

Ten derivatives were assayed for their relative inhibitory potency against NF-κB activation induced by LPS. The results of assay are summarized in Table 1. The inhibition values indicate that entire set of compounds efficiently inhibit the NF-κB

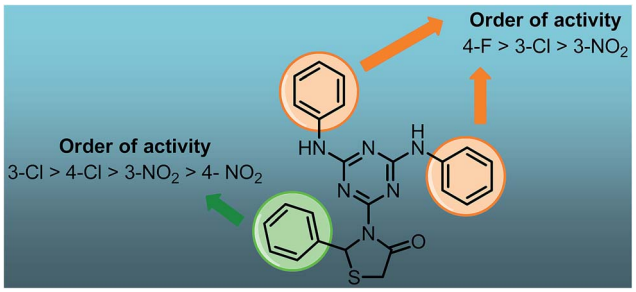

Fig. 4 Structure–activity relationships of hybrid derivatives for NF-κB inhibition.

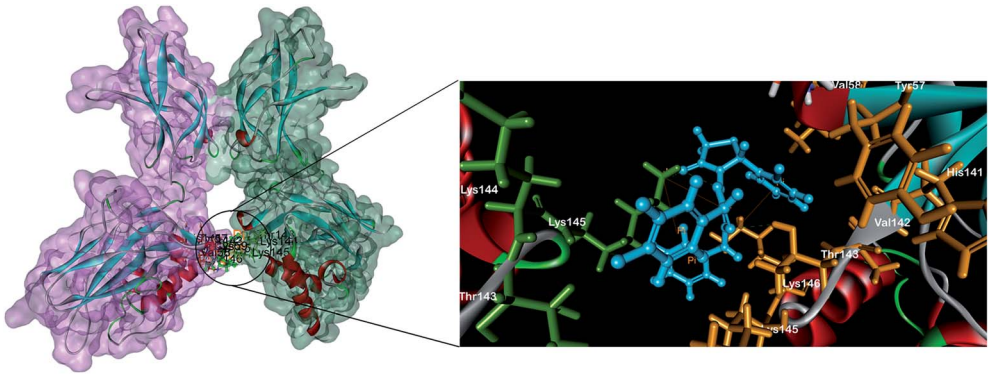

Fig. 5 Docking of SP6 in the active site of p50 NF-κB homodimer, where, A-chain was colored as green and Chain B as violet; whereas in inset, the ligand: blue, A-chain interacting residue: green, B-chain interacting residue: brown.

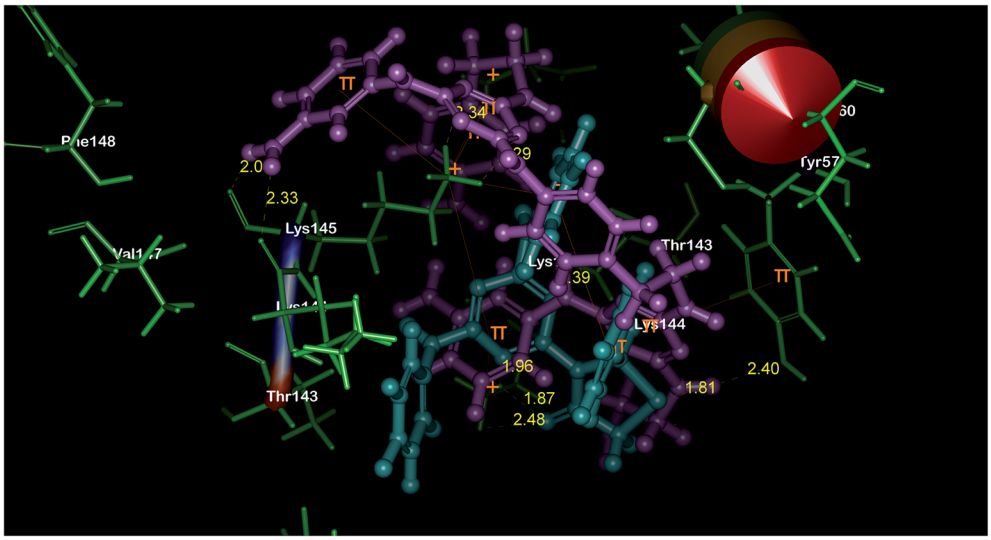

Fig. 6 Docked orientation of compound SP6 (shown in blue) along with PBI-1308 (shown in violet) in the active site of p50 NF-κB homodimer.

activation provoked by LPS. In particular, compounds SP5 and SP6 having fluoro on the phenyl of triazine with isomeric substitution of chloro exhibited excellent NF-κB inhibition (respectively with relative NF-κB activity: 1.82 ± 1.87 and 1.96 ± 1.56). Compounds SP1 and SP2 with chloro substitutions on the both the rings showed minor decreases in activity. The further decline in NF-κB activity was reported by compound SP7 and SP8: 2.74 ± 0.67 and 2.45 ± 0.12, respectively. Compound SP3 and SP4, having isomeric nitro on the phenyl of thiazolidin-4-one exhibited considerable inhibition activity against NF-κB. Moderate activity was disclosed by compounds SP9 and SP10 containing 3-NO_2 on the phenyl of triazine with isomeric chloro (respectively with relative NF-κB activity: 5.12 ± 0.33, 4.77 ± 1.46). In the study, the control group was calculated without stimulated by LPS (with the relative NF-κB activity (NF-κB/TK, fold): 1.22 ± 0.34). Whereas, the LPS group was defined as the stimulated group (with the relative NF-κB activity (NF-κB/TK, fold): 5.15 ± 0.98). Based on the results, the structure–activity relationship (SAR) has been clearly depicted in the Fig. 3.

Table 2 Interaction involved in docking study of compound SP6

Molecule	H-Bond interacting residues	π–π	π–+
SP6	Lys145, Lys146	Tyr57	Lys145, Lys144

Table 3 Antibiofilm activity of hybrid compounds[a]

	Minimum inhibitory concentration (MIC, in μg mL^{-1})	
Compounds	*S. aureus*	*P. aeruginosa*
SP1	62.5	31.25
SP2	125	ND
SP3	62.5	ND
SP4	62.5	62.5
SP5	ND	31.25
SP6	31.25	7.81
SP7	62.5	62.5
SP8	125	62.5
SP9	ND	31.25
SP10	125	31.25
Vancomycin	3.91	7.81

[a] ND – not determined.

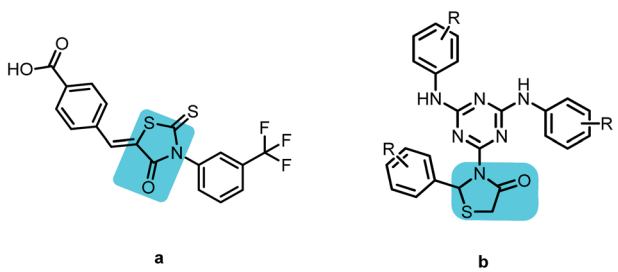

Fig. 7 Structures of compounds. (a) CFTR Inh_{172} (b) target hybrid derivative.

Docking studies

Results showed that, compound SP6 was deeply buried in the DNA binding surface of the N-terminal domains involved in the formation of the solvent-filled cavity, as shown in Fig. 4. It was found that thiazolidine-4-one along with its phenyl, found oriented towards the hydrophobic pocket formed by Tyr57, Val58, Cys59, His141, and Val142. The nitrogen of triazine involved in the formation of two hydrogen bonds with Lys145 and Thr143 of the NF-κB protein model. The formation of another hydrogen bond was revealed by the oxygen of thiazolidin-4-one with Lys145 (Chain A). Moreover, 1,3,5-triazine was involved in a π–π stacking interaction with the aromatic moiety of Tyr57 which is a residue specific for molecular interactions of NF-κB with the DNA sequence 5′-GGGATTTCC-3′ (Chain B). In particular, 1,3,5-triazine ring along with its phenyl stabilized in the active site by a formation of salt bridge with Lys145 (Chain A). Additionally, Lys144 of Chain B was attributed to form another salt bridge with phenyl of 1,3,5-triazine and thiazolidin-4-one, Fig. 5. To further validate the efficiency of docking calculation and interaction with known inhibitor, compound SP-6 was simultaneously docked with PBI-1308, a well known triazine based NF-κB inhibitor. Results revealed that, designed compound SP-6 interacts in similar fashion with PBI-1308 with the involvement of same amino acid residues. The orientation of both ligands has been clearly depicted in Fig. 6 (Table 2).

Antibiofilm activity

P. aeruginosa together with *S. aureus* are the leading cause of the morbidity and mortality of CF patients through recurrent respiratory infections. In our previous studies, these constitutive compounds revealed as highly potent antibacterial agent against *P. aeruginosa*

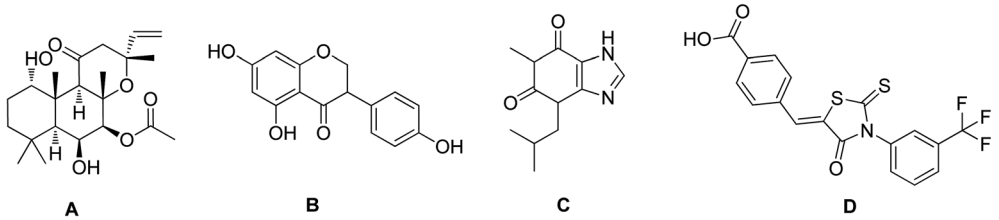

Fig. 8 Structures of compounds used in Micro Ussing chamber studies, where (A): forskolin, (B): IBMX, (C): genistein, (D): CFTR Inh_{172}.

and *S. aureus* in planktonic stage. The generation of drug resistant biofilms of these organisms poses a serious threat to the conventional chemotherapeutics. Therefore, these novel compounds were tested for anti-biofilm activity towards the goal of discovering new anti-infective agents active against microbial biofilms.

As depicted in Table 3, none of the compounds exhibited similar activity against biofilms of *S.aureus vs.* the vancomycin as standard. Compounds SP1, SP3, SP4 and SP7 found to exhibit moderate antibiofilm activity. Moreover, compounds SP2, SP8 and SP10 showed mild antibiofilm activity along with non

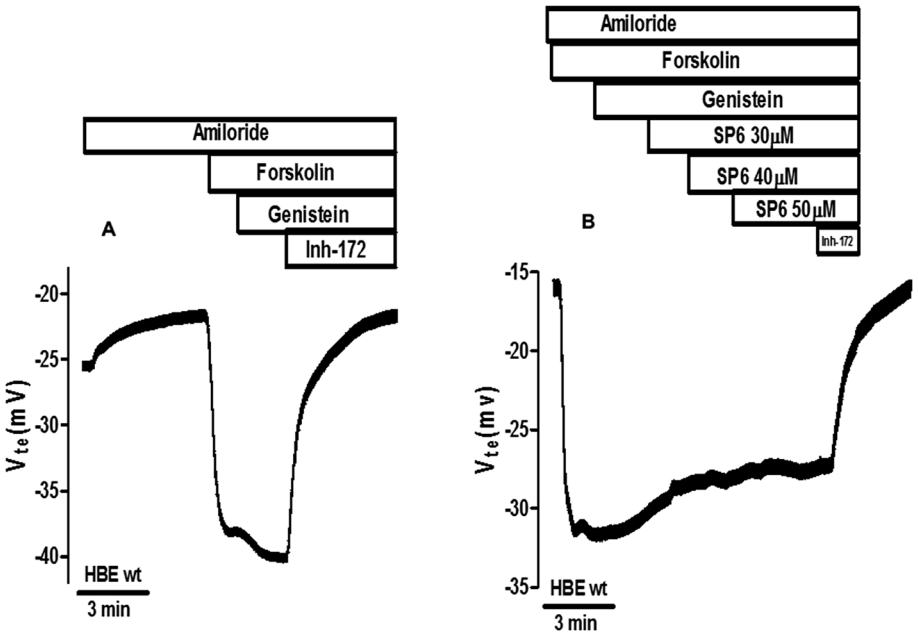

Fig. 9 Original Ussing chamber (open-circuit) recordings obtained for the analyses of monolayers of primary WT HBE cells or CFBE treated with forskolin + IBMX to activate CFTR, followed by genistein to further potentiate the forskolin + IBMX response and treated with (B) SP6 test compound (at 30, 40 and 50 μM concentrations followed by 30 μM CFTR Inh_{172}) which did not inhibit the CFTR-mediated Cl^- currents as CFTR Inh_{172}; or (A) 30 μM Inh_{172} alone which blocks the CFTR-mediated Cl^- currents.

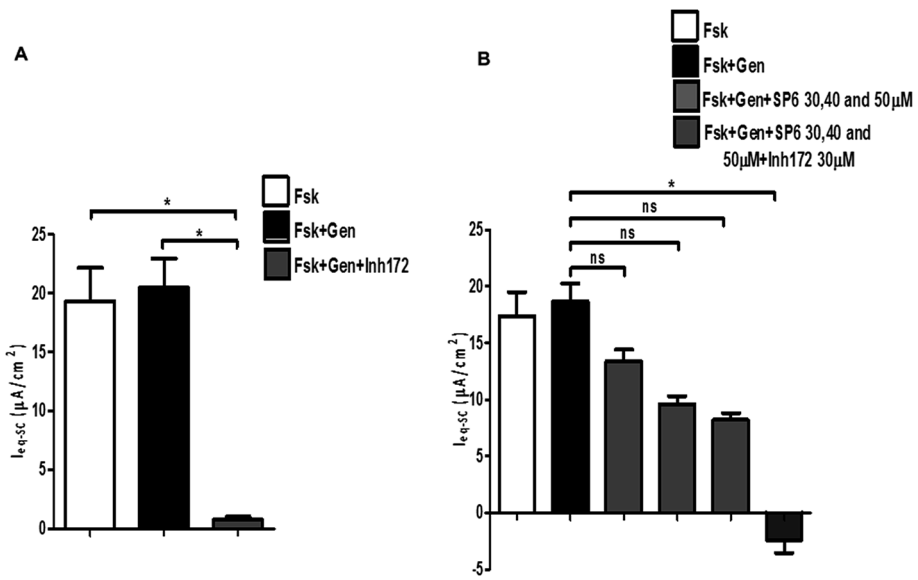

Fig. 10 Summary of Ussing chamber data for the comparative effects of (A) 30 μM CFTR Inh_{172} (grey bar) or (B) SP6 test compound (at 30, 40 and 50 μM concentrations and subsequent effect of 30 μM CFTR Inh_{172}, grey bars) in inhibiting CFTR mediated Cl^- currents in HBE primary cells. Graph represents summary of $I_{sc\text{-}eq}$ (μA cm^{-2}) values obtained for responses to Fsk (white bars) or Fsk + Gen (black bars). Data show that at the tested concentration range, SP6 compound fails to inhibit CFTR as Inh_{172} does. * means significant differences between CFTR-mediated Cl^-currents before and after inhibitor (SP6 or CFTR Inh_{172}) treatment (p value < 0.05 in t-test). n: number of experiments and ns: not significant.

detectable activity by displayed by compounds SP5 and SP9. In the case of *P. aeruginosa*, compounds SP2 and SP3 showed no anti-biofilm activity. It is noteworthy to mention that, compound SP6 showed equipotent activity to vancomycin against *P. aeruginosa*, while rest of the compounds displayed mild to moderate activity.

From the antibiofilm activity data, it became evident that compound SP6 was found more active, while other analogues showed mild to moderate activity against the two tested strains.

Effect on CFTR activity

In high-throughput screening, a thiazolidione based compound 3-[(3-trifluoromethyl)phenyl]-5-[(4-carboxyphenyl)methylene]-2-thioxo-4-thiazolidinone (CFTR Inh_{172}) was previously identified as potent CFTR inhibitor which blocked CFTR chloride (Cl^-) conductance fully with $IC_{50} < 0.5$ μM.[12] Whereas, by comparison of the structures of compounds used in the present study with that of Inh_{172}, it became apparent that both structures share a common pharmacophore, as shown in Fig. 7.

Therefore, the most active compound – SP6 – was evaluated as an inhibitor of the Cystic Fibrosis (CF) Transmembrane Conductance Regulator (CFTR) protein. The efficacy of the compound was determined by its ability to inhibit CFTR-mediated currents. The structures of compounds used in the study have been shown in Fig. 8.

Results show that responses to Fsk and Fsk + Gen in wt HBE′ were 19.30 ± 2.855 and 20.46 ± 2.486 (mean ± SEM μA cm^{-2}), respectively. Subsequent addition of SP6 (at 30, 40 and 50 μM) after Fsk + Gen stimulation, inhibited the current by 13.41 ± 1.007, 9.603 ± 0.699 and 8.217 ± 0.6113, respectively, albeit not significantly. Specific CFTR inhibitor Inh_{172} inhibited the rest of the current completely, which suggests that compound SP6 does not interfere with the binding site of Inh_{172}. In conclusion, no significant change in CFTR-mediated Cl^- currents could be observed for the HBE wt-cells following exposure to SP6 compound, in contrast to the inhibitory effect of these currents observed after Inh_{172}-treatment, Fig. 9 and 10.

Acknowledgements

Authors are thankful to SHIATS for providing necessary infra-structural facilities. Present study has been funded through grant PTDC/SAU-GMG/122299/2010 from FCT/MCTES/PIDDAC (to MDA) and PEst-OE/BIA/UI4046/2011 centre grant (to Bio-ISI, Centre ref. 4046) and PhD fellowship SFRH/BD/94486/2013 from FCT, Portugal (to NTA).

References

1 (*a*) J. M. Rommens, M. C. Iannuzzi, B. Kerem, M. L. Drumm, G. Melmer, M. Dean, R. Rozmahel, J. L. Cole, D. Kennedy, N. Hidaka, M. Zsiga, M. Buchwald, J. R. Riordan, L.-C. Tsui and F. S. Collins, *Science*, 1989, **245**, 1059; (*b*) J. R. Riordan, J. M. Rommens, B. Kerem, N. Alon, R. Rozmahel, Z. Grzelczak, J. Zielenski, S. Lok, N. Plavsic, J. L. Chou, M. L. Drumm, M. C. Iannuzzi, F. S. Collins and L.-C. Tsui, *Science*, 1989, **245**, 1066.

2 (*a*) R. Tirouvanziam, S. de Bentzmann, C. Hubeau, J. Hinnrasky, J. Jacquot, B. Peault and E. Puchelle, *Am. J. Respir. Cell Mol. Biol.*, 2000, **23**, 121; (*b*) C. Verhaeghe, K. Delbecque, L. de Leval, C. Oury and V. Bours, *J. Cystic Fibrosis*, 2007, **6**, 304.

3 (*a*) T. S. Murray, M. Egan and B. I. Kazmierczak, *Curr. Opin. Pediatr.*, 2007, **19**, 83; (*b*) T. F. Murphy, A. L. Brauer, K. Eschberger, P. Lobbins, L. Grove, X. Cai and S. Sethi, *Am. J. Respir. Crit. Care Med.*, 2008, **177**, 853; (*c*) E. E. Smith, D. G. Buckley, Z. Wu, C. Saenphimmachak, L. R. Hoffman, D. A. D'Argenio, S. I. Miller, B. W. Ramsey, D. P. Speert, S. M. Moskowitz, J. L. Burns, R. Kaul and M. V. Olson, *Proc. Natl. Acad. Sci. U. S. A.*, 2006, **103**, 8487.

4 (*a*) N. Maurya, S. Awasthi and P. Dixit, *Indian J. Med. Res.*, 2012, **135**, 469; (*b*) L. A. Clunes, C. M. Davies, R. D. Coakley, A. A. Aleksandrov, A. G. Henderson, K. L. Zeman, E. N. Worthington, M. Gentzsch, S. M. Kreda, D. Cholon, W. D. Bennett, J. R. Riordan, R. C. Boucher and R. l. Tarran, *FASEB J.*, 2102, **26**, 533; (*c*) P. A. Sloane, S. Shastry, A. Wilhelm, C. Courville, L. P. Tang, K. Backer, E. Levin, S. V. Raju, Y. Li, M. Mazur, S. Byan-Parker, W. Grizzle, E. J. Sorscher, M. T. Dransfield and S. M. Rowe, *PLoS One*, 2012, **7**, e39809; (*d*) B. Johannesson, S. Hirtz, J. Schatterny, C. Schultz and M. A. Mall, *PLoS One*, 2012, **7**, e44059; (*e*) M. Bodas, I. Tran and N. Vij, *Curr. Mol. Med.*, 2012, **12**, 807.

5 (*a*) S. Fujii, T. Kobayashi, A. Nakatsu, H. Miyazawa and H. Kagechika, *Chem. Pharm. Bull.*, 2014, **62**, 700; (*b*) M. Neelgundmath, K. R. Dinesh, C. D. Mohan, F. Li, X. Dai, K. S. Siveen, S. Paricharak, D. J. Mason, J. E. Fuchs, G. Sethi, A. Bender, K. S. Rangappa, O. Kotresh and Basappa, *Bioorg. Med. Chem. Lett.*, 2015, **25**, 893; (*c*) V. Pande, R. K. Sharma, J. Inoue, M. Otsuka and M. J. Ramos, *J. Comput.-Aided Mol. Des.*, 2003, **17**, 825.

6 (*a*) B. Singh, H. R. Bhat, M. K. Kumawat and U. P. Singh, *Bioorg. Med. Chem. Lett.*, 2014, **24**, 3321; (*b*) H. R. Bhat, U. P. Singh, P. Gahtori, S. K. Ghosh, K. Gogoi, A. Prakash and R. K. Singh, *New J. Chem.*, 2013, **37**, 2654; (*c*) S. Kumar, H. R. Bhat, M. K. Kumawat and U. P. Singh, *New J. Chem.*, 2013, **37**, 581; (*d*) H. R. Bhat, U. P. Singh, P. Gahtori, S. K. Ghosh, K. Gogoi, A. Prakash and R. K. Singh, *RSC Adv.*, 2013, **3**, 2942–2952; (*e*) U. P. Singh, M. Pathak, V. Dubey, H. R. Bhat and R. K. Singh, *Chem. Biol. Drug Des.*, 2012, **80**, 572–583; (*f*) V. Dubey, M. Pathak, H. R. Bhat and U. P. Singh, *Chem. Biol. Drug Des.*, 2012, **80**, 598; (*g*) P. Gahtori, S. K. Ghosh, P. Pratap, A. Prakash, K. Gogoi, H. R. Bhat and U. P. Singh, *Exp. Parasitol.*, 2012, **130**, 292; (*h*) U. P. Singh, H. R. Bhat and P. Gahtori, *Med. Mycol. J.*, 2012, **22**, 134.

7 H. Sebban and G. Courtois, *Biochem. Pharmacol.*, 2006, **72**, 1153.

8 B. Grouix, M. Lagraoui, M.-E. Fafard, D. Gaudreau, M. Asselin, F. Sarra-Bournet, N. St-Amant, N. Wilb, B. Zacharie, C. Penney and L. Gagnon, *Cancer Res.*, 2008, **68**, 5389.

9 (*a*) I. Vazzana, E. Terranova, F. Mattioli and F. Sparatore, *ARKIVOC*, 2004, 364–374; (*b*) A. Ialenti, G. Grassia, P. Di

Meglio, P. Maffia, M. Di Rosa and A. Ianaro, *Mol. Pharmacol.*, 2005, **67**, 1620; (*c*) B. Goel, T. Ram, R. Tyagi, E. Bansal, A. Kumar, D. Mukherjee and J. N. Sinha, *Eur. J. Med. Chem.*, 1999, **34**, 265; (*d*) S. K. Suthar, V. S. Jaiswal, Lohan, S. Bansal, A. Chaudhary, A. Tiwari, A. T. Alex and A. Joesph, *Eur. J. Med. Chem.*, 2013, **63**, 589.

10 L. Qiu, L. Ding, J. Huang, D. Wang, J. Zhang and B. Guo, *Immunology*, 2009, **128**, 325.

11 (*a*) S. L. Mayo, B. D. Olafson and W. A. Goddard III, *J. Phys. Chem.*, 1990, **94**, 8897; (*b*) B. R. Brooks, R. E. Bruccoleri, B. D. Olafson, D. J. States, S. Swaminathan and M. Karplus, *J. Comput. Chem.*, 1983, **4**, 187; (*c*) F. A. Momany and R. Rone, *J. Comput. Chem.*, 1992, **13**, 888; (*d*) C. M. Venkatachalam, X. Jiang, T. Oldfield and M. Waldman, *J. Mol. Graphics Modell.*, 2003, **21**, 289; (*e*) S. L. Mayo, B. D. Olafson and W. A. Goddard III, *J. Phys. Chem.*, 1990, **94**, 8897.

12 T. Ma, J. R. Thiagarajah, H. Yang, N. D. Sonawane, C. Folli, L. J. Galietta and A. S. Verkman, *J. Clin. Invest.*, 2002, **110**, 1651.

13 M. L. Fulcher and S. H. Randell, *Methods Mol. Biol.*, 2013, **945**, 109.

14 N. T. Awatade, I. Uliyakina, C. M. Farinha, L. A. Clarke, K. Mendes, A. Solé, J. Pastor, M. M. Ramos and M. D. Amaral, *EBioMedicine*, 2014, **2**, 147.

15 S. Moniz, M. Sousa, B. J. Moraes, A. I. Mendes, M. Palma, C. Barreto, J. I. Fragata, M. D. Amaral and P. Matos, *ACS Chem. Biol.*, 2013, **8**, 432.

